

Multicast Group Management for Multi-View 3D Videos in Wireless Networks

Chi-Heng Lin¹, De-Nian Yang¹, Chih-Chung Lin¹ and Wanjiun Liao²

Academia Sinica, Taipei, Taiwan¹

{cchen2008, dnyang, chchlin}@iis.sinica.edu.tw¹

National Taiwan University, Taipei, Taiwan²

wjliao@cc.ee.ntu.edu.tw²

Abstract—With the emergence of naked-eye 3D mobile devices, mobile 3D video services become increasingly important for video service providers, such as Youtube and Netflix, while multi-view 3D videos are potential to bring out varied innovative applications. However, enabling multi-view 3D video services may overwhelm WiFi networks when we multicast every view of a video. In this paper, therefore, we propose to incorporate depth-image-based rendering (DIBR), which allows each mobile client to synthesize the desired view from nearby left and right views, to effectively reduce the bandwidth consumption. Moreover, due to varied channel conditions, each client may suffer from different packet loss probabilities, and retransmissions incur additional bandwidth consumption. To address this issue, we first analyze the merit of view protection via DIBR for multi-view video multicast and then design a new protocol, named Multi-View Group Management Protocol (MVGMP), for the dynamic group management of multicast users. Simulation results manifest that our protocol effectively reduces the bandwidth consumption and increases the probability for each client to successfully playback the desired view of a multi-view 3D video.

Index Terms—3D Video, WiFi, Multi-View, DIBR, View Loss

I. INTRODUCTION

The IEEE 802.11 [1] WiFi standard has achieved massive market penetration due to its low cost, easy deployment and high bandwidth. Also, with the recent emergence of naked-eye 3D mobile devices, such as Amazon's 3D Fire Phone, HTC's EVO 3D, LG's Optimus 3D, and Sharp's Lynx, mobile 3D video services are expected to become increasingly important for video service providers, such as Youtube and Netflix. In contrast to traditional stereo single-view 3D video formats, multi-view 3D videos provide users with a choice of viewing angles and thus are expected to inspire the development of innovative applications in television, movies, education, and advertising [2]. Previous researches on the deployment of 3D videos in wireless networks mostly focused on improving 3D video quality for single-view 3D videos [3], [4], [5]. Nevertheless, multi-view 3D videos, which typically offer 16 different viewing angles [6], are expected to significantly increase the network load when all views are transmitted.

One promising way to remedy the bandwidth issue is by exploiting depth-image-based rendering (DIBR) in mobile clients. Because adjacent views usually share many similar parts, a user's desired view can be synthesized from nearby left and right views [2]. Several schemes for bit allocation between the texture and depth map [7], [8] and rate con-

trol with layered encoding for a multi-view 3D video [9], [10] have been proposed to ensure that the quality of the synthesized view is very close to the original view (i.e., by minimizing total distortion or maximizing quality). Therefore, exploiting DIBR in clients eliminates the requirement to deliver each view of a multi-view video if the left and right views of the desired view have been transmitted to other clients. Moreover, the computation overhead incurred by DIBR is small enough to be handled by current mobile devices [10], [11].

However, multi-view 3D video multicast with DIBR brings new challenges in WiFi networks. 1) The number of views between the left and right transmitted views needs to be constrained to ensure the quality of the synthesized view [2]. In other words, since each transmitted view is shared by multiple clients, one must carefully select the transmitted views so that the desired view of each user can be synthesized with good quality. DIBR has a quality constraint [2], which specifies that the left and right views are allowed to be at most R views away (i.e., $R-1$ views between them) to ensure that every view between the left and right view can be successfully synthesized with good quality. Therefore, each new user cannot arbitrarily choose a left and a right view for synthesis with DIBR. 2) WiFi networks frequently suffer from wireless erasure, and different clients suffer from different loss probabilities due to varying channel conditions [12], [13], [14], [15]. In 2D and single-view 3D videos, the *view loss probability* for each user can be easily derived according to the corresponding channel state information. The view loss probability for each user is correlated to the selected bit-rate, channel, and the setting of MIMO (ex. antennas, spatial streams) in 802.11 networks. For multi-view 3D videos, however, when a video frame is lost for a user i subscribing a view k_i , the left and right views multicasted in the network for other users can natively serve to *protect* view k_i , since the user i can synthesize the desired view from the two views using DIBR. However, the view synthesis will fail if only one left view or one right view is received successfully by the client. Therefore, a new research problem is to find out the *view failure probability*, which is the probability that each user doesnot successfully receive and synthesize his/her desired view.

In this paper, therefore, we first analyze the merits of DIBR for multi-view 3D video multicast in multi-rate multi-channel WiFi networks [1]. We analyze the view failure probability for comparison with the traditional view loss

probability. We then propose Multi-View Group Management Protocol (MVGMP) for multi-view 3D multicast. When a user joins the video multicast group, it can exploit our analytical results to request the AP to transmit the most suitable right and left views, so that the view failure probability is guaranteed to stay below a threshold. On the other hands, when a user leaves the video multicast group, the proposed protocol carefully selects and withdraws a set of delivered views to reduce the network load, so that the video failure probability for other users will not exceed the threshold. Bandwidth consumption can be effectively reduced since not all subscribed views are necessary to be delivered. Moreover, the protocol supports the scenario in which each user subscribes to multiple desired views.

The rest of the paper is organized as follows. Section II describes the system model. Section III analyzes the view loss probability and view failure probabilities. Section IV presents the proposed protocol. Section V shows the simulation results, and Section VI concludes this paper.

II. SYSTEM MODEL

This paper considers the single-cell point-to-multipoint video transmissions in IEEE 802.11 networks, where the views transmitted by different bit-rates and on different channels are associated with different loss probabilities [16], [12], [13], [14], [15]. Currently, many video services, such as Youtube and Netflix, require reliable transmissions since Flash or MPEG DASH [17] are exploited for video streaming. Nevertheless, the current IEEE 802.2 LLC protocol for IEEE 802.11 networks does not support reliable multicast transmissions [18], and error recovery thereby needs to be handled by Layer-3 reliable multicast standards, such as PGM [19].

A 3D video in multi-view plus depth can be encoded by varied encoding schemes [20], [21]. The idea of DIBR is to infer and synthesize the parts different from nearby views, while effective techniques are proposed to ensure the video quality [22], [23]. In the original WiFi multicast without DIBR, AP separately multicasts each view to the clients. By contrast, a desired view can be synthesized by nearby left and right views with DIBR, while the quality constraint in DIBR states that there are at most $R - 1$ views between the left and right views, and R can be set according to [2]. In addition, when the subscribed view is lost for a user, the user can also try to synthesize the view according to the left view and right view. In the next section, we investigate the merits of DIBR by analyzing the view failure probability for comparison with the traditional view loss probability.

III. ANALYTICAL SOLUTION

In this section, we present the analytical results for multi-rate multi-channel IEEE 802.11 networks with DIBR. We first study the scenario of single-view subscription for each client and then extend it to multi-view subscription. Table I summarizes the notations in the analysis. Based on the mathematical analysis, a new protocol is proposed in the next section to adaptively assign the proper views to each client.

TABLE I
NOTATIONS.

Description	Notation
R	Quality constraint of DIBR
M	Total number of views which can be selected
k_i	The k view selected by user i
D_i	A set of the available data rates for user i
C_i	A set of the available channels for user i
$n_{j,c,r}$	Number of broadcasts for the j view transmitted by the r rate in the c channel within a reasonable frame time T_f
$p_{i,c,r}$	The loss probability for user i under the c channel and the r rate
$P_\varepsilon^{(i)}$	The probability that user i cannot obtain his/her selected view either by direct reception or by DIBR
$p_{c,r}^{\text{AP}}(n)$	The probability that AP broadcasts a view by n times under the channel c and the rate r
α_i	The probability of the selected view obtained by user i
η_i	Minimum retransmission rate for user i
p_{select}	The probability that an user selects a certain view

A. Single View Subscription

In single-view subscription, each user i specifies only one desired view k_i . Each view can be sent once or multiple times by the AP. Let $p_{i,c,r}$ represent the *view loss probability*¹, which is the probability that user i does not successfully receive a view under the channel c and the data rate r . We define a new probability $P_\varepsilon^{(i)}$ for multi-view 3D videos, called *view failure probability*, which is the probability that user i fails to receive or synthesize his desired view because the desired view and nearby left and right views for synthesis with DIBR are all lost. In other words, the view loss probability considers only one view, while the view failure probability jointly examines the loss events of multiple views.

Theorem 1. *For single-view subscription, the view failure probability for user i is*

$$\begin{aligned}
 P_\varepsilon^{(i)} = & \prod_{c \in C_i, r \in D_i} p_{i,c,r}^{n_{k_i,c,r}} \times \\
 & \left[\mathbf{1}\{k_i = 1\} + \mathbf{1}\{k_i = M\} + \right. \\
 & \sum_{k=1}^{R-1} \left(\left(1 - \prod_{c' \in C_i, r' \in D_i} p_{i,c',r'}^{n_{k_i-k,c',r'}} \right)^{\min(R-k, M-k_i)} \prod_{l=1}^{k-1} \prod_{\substack{r_1, r_2 \in D_i \\ c_1, c_2 \in C_i}} \right. \\
 & \left. \prod_{q=1}^{k-1} p_{i,c_1,r_1}^{n_{k_i-q,c_1,r_1}} p_{i,c_2,r_2}^{n_{k_i+q,c_2,r_2}} \mathbf{1}\{M-1 \geq k_i \geq k+1\} \right) + \\
 & \left. \prod_{q=1}^{\min(R-1, k_i-1)} \prod_{c_3 \in C_i, r_3 \in D_i} p_{i,c_3,r_3}^{n_{k_i-q,c_3,r_3}} \mathbf{1}\{M-1 \geq k_i \geq 2\} \right]
 \end{aligned}$$

where $\mathbf{1}\{\cdot\}$ denotes the indicator function.

Proof: The view failure event occurs when one of the following two conditions holds: 1) user i does not successfully receive his/her desired view, and 2) user i fails to receive any feasible set of a left view and a right view with the

¹Many data frames in layer-2 aggregate one view. Thus, the loss probability of each loss frame forms the view loss probability.

view distance at most R to synthesize the desired view. The probability of the first condition is $\prod_{c \in C_i, r \in D_i} p_{i,c,r}^{n_{k_i,c,r}}$ when the desired view k_i of user i is transmitted by n_{k_i} times. Note that if the desired view of user i is view 1 or view M , i.e., $k_i = 1$ or $k_i = M$, user i is not able to synthesize the desired view with DIBR, and thus the view failure probability can be directly specified by the first condition. For every other user i with $M-1 \geq k_i \geq 2$, we define a set of non-overlapping events $\{\mathcal{B}_k\}_{k=0}^{R-1}$, where \mathcal{B}_k with $k > 0$ is the event that the nearest left view received by user i is $k_i - k$, but user i fails to receive a feasible right view to synthesize the desired view. On the other hand, \mathcal{B}_0 is the event that the user i fails to receive any left view. Therefore, $\bigcup_{k=0}^{R-1} \mathcal{B}_k$ jointly describes all events for the second condition.

Since the two events described above are independent, we can derive their probabilities separately and then multiply them together to obtain the view failure probability for the user i .

For each event \mathcal{B}_k with $k > 0$,

$$P(\mathcal{B}_k) = (1 - \prod_{c' \in C_i, r' \in D_i} p_{i,c',r'}^{n_{k_i-k,c',r'}})^{\min(R-k, M-k_i)} \prod_{l=1}^{\min(R-k, M-k_i)} \prod_{\substack{r_1, r_2 \in D_i \\ c_1, c_2 \in C_i}} \prod_{q=1}^{k-1} p_{i,c_1,r_1}^{n_{k_i-q,c_1,r_1}} p_{i,c_2,r_2}^{n_{k_i+l,c_2,r_2}} \mathbf{1}\{M-1 \geq k_i \geq k+1\}$$

The first term $1 - \prod_{c' \in C_i, r' \in D_i} p_{i,c',r'}^{n_{k_i-k,c',r'}}$ represents that user i successfully received view $k_i - k$, and the second term

$$\prod_{l=1}^{\min(R-k, M-k_i)} \prod_{\substack{r_1, r_2 \in D_i \\ c_1, c_2 \in C_i}} \prod_{q=1}^{k-1} p_{i,c_1,r_1}^{n_{k_i-q,c_1,r_1}} p_{i,c_2,r_2}^{n_{k_i+l,c_2,r_2}}$$

describes that user i does not successfully receive any left view between $k_i - k$ and k and any right view from $k_i + 1$ to $k_i + \min(R-k, M-k_i)$. It is necessary to include a indicator function in the last term since \mathcal{B}_k will be a null event if $k_i \leq k$, i.e., user i successfully receives a view outside the view boundary. Finally, the event \mathcal{B}_0 occurs when no left view successfully received by user i .

$$P(\mathcal{B}_0) = \prod_{q=1}^{\min(R-1, k_i-1)} \prod_{c_3 \in C_i, r_3 \in D_i} p_{i,c_3,r_3}^{n_{k_i-q,c_3,r_3}} \mathbf{1}\{M-1 \geq k_i \geq 2\}$$

The theorem follows after summarizing all events. ■

Remark: The merit of multi-view 3D multicast with DIBR can be unveiled by comparing the view loss probability and view failure probability. The view failure probability attaches a new term (i.e., the probability of $\bigcup_{k=0}^{R-1} \mathcal{B}_k$) with the value at most 1 to the view loss probability, while a larger R leads to a smaller probability.

B. Multiple View Subscription

In the following, we explore the case that a user desires to subscribe multiple views. We study the following two scenarios: 1) every view is multicasted; 2) only one view is

delivered for every \tilde{R} views, $\tilde{R} \leq R$, and thus it is necessary for a user to synthesize other views accordingly. We first define α_i , which represents the percentage of desired views that can be received or synthesized by user i successfully.

$$\alpha_i = \frac{\sum_{k_i \in \mathcal{K}_i} \mathbf{1}\{\text{user } i \text{ can obtain view } k_i\}}{|\mathcal{K}_i|}$$

where \mathcal{K}_i denotes the set of desired views for user i . Since retransmission is necessary to be involved when a desired view cannot be received or synthesized, we derive the minimal number of views required to be retransmitted to obtain all desired views for each user later in [24]. By using Theorem 1, we can immediately arrive at the following corollary.

Corollary 1.

$$\mathbb{E}[\alpha_i] = \frac{\sum_{k_i \in \mathcal{K}_i} P_\varepsilon^{(i)}(k_i)}{|\mathcal{K}_i|} \quad (1)$$

where $P_\varepsilon^{(i)}(k_i)$ is given in Theorem 1.

Proof:

$$\begin{aligned} \mathbb{E}[\alpha_i] &= \frac{\sum_{k_i \in \mathcal{K}_i} \mathbb{E}\mathbf{1}\{\text{user } i \text{ can obtain view } k_i\}}{|\mathcal{K}_i|} \\ &= \frac{\sum_{k_i \in \mathcal{K}_i} P_\varepsilon^{(i)}(k_i)}{|\mathcal{K}_i|} \end{aligned}$$

■

Eq. (1) becomes more complicated as $|\mathcal{K}_i|$ increases. In the following, therefore, we investigate asymptotic behavior α_i for a large $|\mathcal{K}_i|$ and also a large M since $|\mathcal{K}_i| \leq M$. To find the closed-form solution, we first consider uniform view subscription and assume that user i subscribes each view j with probability $p_{\text{select}} = \frac{|\mathcal{K}_i|}{M}$ independently across all views so that the average number of selected views is $|\mathcal{K}_i|$. Assume the AP multicasts view j in channel c with rate r by n times with probability $p_{j,c,r}^{\text{AP}}(n)$ independently across all views, channels, and rates. Although a multi-view 3D videos usually contains only dozens of views, Section V manifests that the asymptotic analysis result is very close to the result in Theorem 2. The theoretical result is first summarized in the following theorem where we fix p_{select} and let $|\mathcal{K}_i| \rightarrow \infty$, and we then present the insights from the theorem by comparing the results of single-view subscription and multi-view subscription. Due to the space constraint, a more general analysis that also allows each user to subscribe a sequence of consecutive views is presented in [24].

Theorem 2. *In multi-view subscription,*

$$\alpha_i(\mathcal{K}_i) \xrightarrow{a.s.} (1 - p_i) \left\{ \sum_{k=1}^R k(1 - p_i) p_i^{k-1} + p_i^R \right\} \quad (2)$$

$$\mathbb{E}[\alpha_i(\mathcal{K}_i)] \xrightarrow{a.s.} (1 - p_i) \left\{ \sum_{k=1}^R k(1 - p_i) p_i^{k-1} + p_i^R \right\} \quad (3)$$

as $|\mathcal{K}_i| \rightarrow \infty$, where $p_i = \prod_{c \in C_i, r \in D_i} \sum_n p_{c,r}^{\text{AP}}(n) p_{i,c,r}^n$

Proof: We first derive the view loss probability for user i . Suppose that the AP multicasts a view by n times via

channel c and rate r . The probability that user i cannot successfully receive the view is $p_{i,c,r}^n$. Because the AP will multicast a view by n times via channel c and rate r with probability $p_{c,r}^{\text{AP}}(n)$, the probability that user i cannot receive the view via channel c and rate r is $\sum_n p_{c,r}^{\text{AP}}(n)p_{i,c,r}^n$. Therefore, the view loss probability for user i is the multiplication of the view loss probabilities in all channels and rates, i.e., $\prod_{c \in C_i, r \in D_i} \sum_n p_{c,r}^{\text{AP}}(n)p_{i,c,r}^n$. For simplification, we denote p_i as the view loss probability for user i in the remaining of proof.

Since the multicast order of views is not correlated to α_i , we assume that the AP multicasts the views from view 1 to view M sequentially. Now the scenario is similar to a tossing game, where we toss M coins, a face-up coin represents a view successfully receiving from the AP, thus the face-up probability of coin is $1 - p_i$. Now we mark a coin with probability p_{select} if it is face-up or if there are one former tossed face-up coin and one latter tossed face-up coin with the view distance at most R . Since the above analogy captures the mechanism of direct reception and DIBR of views, the marked coins then represent the views selected by user i that can also be successfully obtained by him.

To derive the closed-form asymptotical result, we exploit the delayed renewal reward process, in which a cycle begins when a face-up coin appears, and the cycle ends when the next face-up coin occurs. The reward is defined as the total number of marked coins. Specifically, let $\{N(t) := \sup\{n : \sum_{i=0}^n X_i \leq t\}, t \geq 0\}$ denote the delayed renewal reward process with interarrival time X_n , where X_n with $n \geq 1$ is the time difference between two consecutive face-up coins, and X_0 is the time when the first face-up coin appears.

Let $R(M)$ and R_n denote the total reward earned at the time M , which corresponds to the view numbers in a multi-view 3D video. At cycle n ,

$$\frac{R(M)}{M} = \frac{\sum_{n=1}^{N(M)} R_n}{M} + o(1) \quad a.s.$$

where the $o(1)$ term comes from the fact that the difference between total reward and $\sum_{n=1}^{N(M)} R_n$ will have a finite mean. Recall that the reward earned at each cycle is the number of marked coins,

$$\mathbb{E}[R_n | X_n] = \begin{cases} p_{\text{select}}, & \text{for } X_n > R \\ X_n p_{\text{select}}, & \text{for } X_n \leq R \end{cases} \quad (4)$$

since when $X_n \leq R$, there are X_n coins can be marked (each marked with probability p_{select}) between two consecutive face-up coins, so the expectation of reward given X_n is $X_n p_{\text{select}}$. By contrast, only one coin can be marked with probability p_{select} when $X_n > R$, so the expectation of reward given X_n is only p_{select} .

Since X_n is a geometric random variable with parameter p , we have

$$\mathbb{E}[X_n] = 1 - p_i + 2(1 - p_i)p_i^2 + 3(1 - p_i)p_i^3 + \dots = \frac{1}{1 - p_i}$$

and

$$\begin{aligned} \mathbb{E}[R_n] &= p_{\text{select}}p_i(1 - p_i) + 2p_{\text{select}}p_i(1 - p_i)^2 + \dots \\ &\quad + Rp_{\text{select}}(1 - p_i)p_i^{R-1} + p_{\text{select}}p_i^R \end{aligned} \quad (5)$$

By theorem 3.6.1 of renewal process in [25],

$$\begin{aligned} \frac{\sum_{n=1}^{N(M)} R_n}{M} &\xrightarrow{a.s.} \frac{\mathbb{E}R_n}{\mathbb{E}X_n} \\ &= p_{\text{select}}(1 - p_i) \left\{ \sum_{k=1}^R k(1 - p_i)p_i^{k-1} + p_i^R \right\} \end{aligned} \quad (6)$$

Let U_M denote the number of views selected by user i , we can write

$$\alpha_i = \frac{R(M)}{U_M} = \frac{R(M)}{M} \frac{M}{U_M}$$

For $\frac{U_M}{M} \xrightarrow{a.s.} p_{\text{select}}$, by the strong law of large number, after combining with Eq. (4), (5), (6),

$$\alpha_i \xrightarrow{a.s.} (1 - p_i) \left\{ \sum_{k=1}^R k(1 - p_i)p_i^{k-1} + p_i^R \right\}$$

The proof for convergence in mean is similar, it is only necessary to replace convergence in Eq. (6) by the convergence in mean, which is guaranteed by the same theorem. ■

Remark: Under the above uniform view subscription, we see that α_i is actually irrelevant to p_{select} which implies that different users with different number of subscription will obtain the same percentage of views they select. Most importantly, $\alpha_i = 1 - p_i$ for multi-view 3D multicast without DIBR. In contrast, multi-view 3D multicast without DIBR effectively improves α_i by $\sum_{k=1}^R k(1 - p_i)p_i^{k-1} + p_i^R$. Since this term is strictly monotonically increasing with R , we have $\sum_{k=1}^R k(1 - p_i)p_i^{k-1} + p_i^R > \sum_{k=1}^1 k(1 - p_i)p_i^{k-1} + p_i = 1$, which implies the percentage of obtained views is strictly larger in statistic by utilizing DIBR technique.

In the following, we consider the second case with only one view delivered for every \tilde{R} views, where the bandwidth consumption can be effectively reduced. Note that the following corollary is equivalent to Theorem 2 when $\tilde{R} = 1$.

Corollary 2. *If the AP only transmits one view with probability $p_{c,r}^{\text{AP}}(n)$ for every \tilde{R} views,*

$$\alpha_i(\mathcal{K}_i) \xrightarrow{a.s.} \frac{(1 - p_i) \left\{ \sum_{k=1}^{\lfloor \frac{R}{\tilde{R}} \rfloor} \tilde{R}k(1 - p_i)p_i^{k-1} + p_i^{\lfloor \frac{R}{\tilde{R}} \rfloor} \right\}}{\tilde{R}} \quad (7)$$

$$\mathbb{E}[\alpha_i(\mathcal{K}_i)] \rightarrow \frac{(1 - p_i) \left\{ \sum_{k=1}^{\lfloor \frac{R}{\tilde{R}} \rfloor} \tilde{R}k(1 - p_i)p_i^{k-1} + p_i^{\lfloor \frac{R}{\tilde{R}} \rfloor} \right\}}{\tilde{R}} \quad (8)$$

as $|\mathcal{K}_i| \rightarrow \infty$, where $p_i = \prod_{c \in C_i, r \in D_i} \sum_n p_{c,r}^{\text{AP}}(n)p_{i,c,r}^n$

Due to the space constraint, the proof is presented in [24].

IV. PROTOCOL DESIGN

Our protocol MVGMP extends the current IETF Internet standard for multicast group management, IGMP [26], by adding the view selection feature to the protocol, while each client selects one view or a set of views according to the analytical results in Section III. IGMP is a receiver-oriented

protocol, where each user periodically and actively updates its joining multicast groups to the designated router (i.e., the AP in this paper). Due to the space constraint, this section only summarizes the behavior of our protocol, and detailed operation can be founded in [24].

For a multi-view 3D video, each view is delivered to a multicast group since users can receive different sets of views. The AP maintains a table, named *ViewTable*, for each video. The table specifies the current multicast views and the corresponding bit-rates and channels for each view², and each multicast view is associated with a multicast address and a set of users that choose to receive the view. *ViewTable* is periodically broadcasted to all users in the WiFi cell. MVGMP includes the following control messages. 1) Join: A Join message contains the address of a new user and the corresponding requested view(s), which can be the subscribed views, or the left and right views to synthesize the subscribed view. An existing user also exploits this message to update its requested views. 2) Leave: A Leave message includes the address of a leaving user and the views that are no longer necessary to be received. An existing user can also exploit this message to stop receiving a view. Following the design rationale of IGMP, MVGMP is also a soft-state protocol, which implies that each user is required to periodically send the Join message to refresh its chosen views, so that unexpected connection drops will not create dangling states in *ViewTable*.

Join. When a new member decides to join a 3D video multicast transmission, it first acquires the current *ViewTable* from the AP. Afterward, the user identifies the views to be received according to Theorem 1. Specifically, the client first examines whether *ViewTable* has included the subscribed view. If *ViewTable* does not include the subscribed view, or if the view loss probability for the subscribed view in the corresponding channel and bit-rate exceeds the threshold, the user adds a left view and a right view that lead to the maximal decrement on the view failure probability. The above process is repeated until the view failure probability does not exceed the threshold.

When a multi-view 3D video starts, usually the current multicast views in *ViewTable* are not sufficient for a new user. In other words, when the view failure probability still exceeds the threshold after the user selects all transmitted left and right views within the range R in *ViewTable*, the user needs to add the subscribed view to *ViewTable* with the most suitable channel and bit-rate to reduce the view failure probability. Also, the left and right views are required to be chosen again to avoid receiving too many views. After choosing the views to be received, a Join message is sent to the AP. The message contains the views, which the user chooses to receive, and the AP adds the user to the *ViewTable* accordingly. To avoid receiving too many views, the client can restrict the maximum number of left and right views that are allowed to be received and exploited for DIBR.

Leave and View Re-organization. On the other hand,

when a user decides to leave a 3D video multicast transmission, it multicasts a Leave message to the AP and any other user that receives at least one identical view k_i . Different from the Join message, the Leave message is also delivered to other staying users in order to minimize the bandwidth consumption, since each staying user that receives k_i will examine if there is a chance to switch k_i to another view \bar{k}_i that is still transmitted in the network. In this case, the staying user also sends a Leave message that includes view k_i , together with a Join message that contains view \bar{k}_i . If a view is no longer required by any staying users, the AP stops delivering the view. Therefore, MVGMP can effectively reduce the number of multicast views. Due to the space constraint, an illustrative example is presented in [24].

Discussion. Note that MVGMP can support the scenario that a user changes the desired view, by first sending a Leave message and then a Join message. Similarly, when a user moves and thus the channel condition changes, it will send a Join message to receive additional views if the channel condition deteriorates, or a Leave message to stop receiving some views if the channel condition improves. Moreover, when a user handovers to a new WiFi cell, it first sends a Leave message to the original AP and then a Join message to the new AP. If the network connection to a user drops suddenly, the AP removes the information corresponding to the user in *ViewTable* when it does not receive the Join message (for soft-state update explained early in this section) for a period of time. Therefore, MVGMP also supports the silent leave of a user from a WiFi cell. Moreover, our protocol can be extended to the multi-view subscription for each client by replacing Theorem 1 with Theorem 2. The fundamental operations of Join/Leave/Reorganize remain the same since each view is maintained by a separate multicast group. Due to the space constraint, an illustrative example of MVGMP is presented in [24].

V. SIMULATION RESULTS

In the following, we first describe the simulation setting and then compare MVGMP with the current multicast scheme.

A. Simulation Setup

In this section, we evaluate the channel time of MVGMP in a series of scenarios in NS3 with 802.11n program package. The channel time of a multicast scheme is the average time consumption of a frame. To the best knowledge, there is no related work on channel time minimization for multi-view 3D video multicast in WiFi networks. Thus, we compare MVGMP with the original WiFi multicast scheme, in which all desired views are multicasted to the users. We adopt the setting of a real multi-view 3D dataset, Book Arrival [6] with 16 views, i.e., $|V| = 16$. Each user randomly chooses one preferred view from three preference distributions: Uniform, Zipf, and Normal distributions. There is no specifically hot view in Uniform distribution. By contrast, Zipf distribution, $f(k; s; N) = (\frac{1}{k^s}) / \sum_{n=1}^N N(\frac{1}{n^s})$, differentiates the desired views, where k is the preference rank of a view, s is the the exponent characterizing the distribution, and N is the number of views. The views with smaller ranks are major

²Note that each view is allowed to be transmitted multiple times in different channels and rates if necessary, as described in Section III.

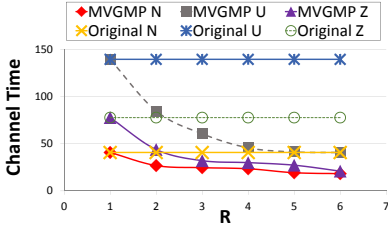


Fig. 1. Synthesis Range

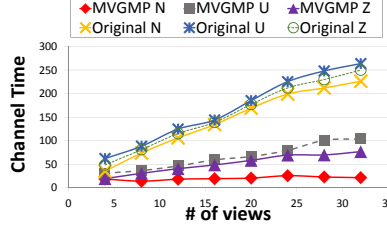


Fig. 2. Number of Views in a Video

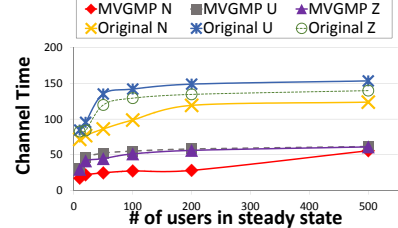


Fig. 3. Number of Users

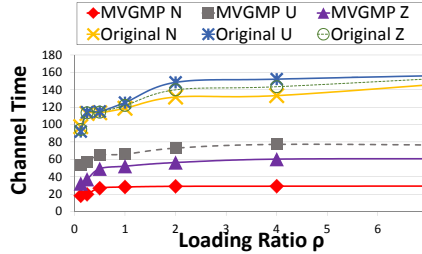


Fig. 4. Network Load

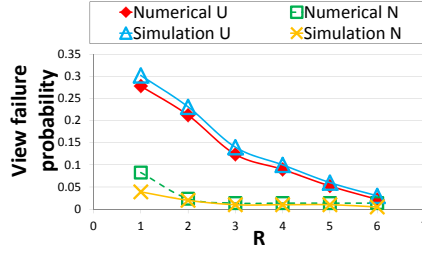


Fig. 5. View Failure Probability

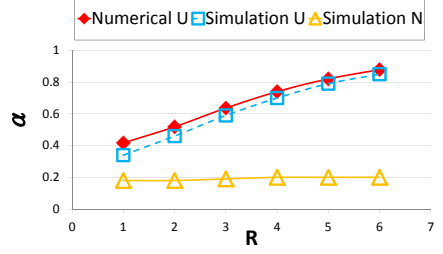


Fig. 6. Ratio of Successfully Received Views

TABLE II
SIMULATION SETTINGS.

Parameter	Value
Carrier Frequency	5.0 GHz
The unit of Channel Time	$10^{-3}ms$
Channel Bandwidth	40MHz
AP Tx Power	16.dBm
OFDM Data Symbols	7
Subcarriers	108
View Size (per 3D video)	64kbits
Number of Orthogonal Channels	2
Data Rates	8 different values defined in 802.11n spec. [1]

views and thus more inclined to be requested. We set $s = 2$ and $N = 16$ in this paper. In Normal distribution, the mean is set as 0.5, and the variance is set as 1 throughout this paper.

We simulate a dynamic environment with 50 client users locating randomly in the range of an AP. After each frame, there will be an arrival and departure of a user with probabilities λ and μ , respectively. In addition, a user will change the desired view with probability η . The default probabilities are $\lambda = 0.2$, $\mu = 0.3$, $\eta = 0.4$. TABLE II summarizes the simulation setting consisting of an 802.11n WiFi network with 40MHz channel bandwidth and two orthogonal channels. In the following, we first compare the performance of MVGMP with the current WiFi multicast scheme in different scenarios and then compare the analytical and simulation results.

B. Scenario: Synthesized Range

Fig. 1 evaluates MVGMP with different settings of R . As expected, the channel time is efficiently reduced as R increases. Nevertheless, it is not necessary to set a large R because the improvement becomes marginal as R exceeds 3. Therefore, the result indicates that a small R (i.e., limited quality degradation) is sufficient to effectively reduce the channel time in WiFi.

C. Scenario: Number of Views

Fig. 2 explores the impact on the numbers of views in a video. The channel time in both schemes increases when the

video includes more views, because more views are necessary to be transmitted. The result manifests that MVGMP consistently outperforms the original WiFi multicast scheme with different numbers of views in a video.

D. Scenario: Number of Users in Steady State

Fig. 3 evaluates the channel time with different numbers of users in the steady state. We set $\lambda = \mu = 0.25$, so that the expected number of users in the network remains the same. The channel time grows as the number of users increases. Nevertheless, the increment becomes marginal since most views will appear in *ViewTable*, and thus more users will subscribe the same views in the video.

E. Scenario: Utilization Factor

Fig. 4 explores the impact of the network load. Herein, we change the *loading ratio* $\rho := \frac{\lambda}{\mu}$, i.e., the ratio between arrival probability λ and departure probability μ , from 0.125 to 8. The results manifest that the channel time is increased for both multicast schemes. Nevertheless, MVGMP effectively reduces at least 40% of channel time for all the three distributions.

F. Impact of User Preferences

From Fig. 1 to Fig. 4, the results manifest that Uniform distribution requires the most channel time compared with Normal distribution. This is because in Normal distribution users prefer a few central front views and thus has a large probability of being synthesized with two views in range R .

G. Analytical Result

Fig. 5 and Fig. 6 compare the simulation results from NS3 and the analytical results of Theorem 1 and Theorem 2, where each client subscribes all views in Fig. 6. The results show that the discrepancy among the simulation and analysis is very small. Most importantly, α increases for a larger R since each user can synthesize and acquire a desired view from more candidate right and left views when the view is lost.

Ex: m=5

Subscription probability

$\frac{c}{1^s}$	$\frac{c}{2^s}$	$\frac{c}{3^s}$	$\frac{c}{4^s}$	$\frac{c}{5^s}$	$\frac{c}{1^s}$	$\frac{c}{2^s}$	$\frac{c}{3^s}$	$\frac{c}{4^s}$	$\frac{c}{5^s}$
-----------------	-----------------	-----------------	-----------------	-----------------	-----------------	-----------------	-----------------	-----------------	-----------------



Successful received views

Fig. 7. Example of consecutive view subscription scenario

VI. CONCLUSIONS

With the emergence of naked-eye mobile devices, this paper proposes to incorporate DIBR for multi-view 3D video multicast in WiFi networks. We first investigate the merits of view protection via DIBR and show that the view failure probability is much smaller than the view loss probability, while multi-view subscription for each client is also studied. Afterward, we propose Multi-View Group Management Protocol (MVGMP) to handle the dynamic join and leave for a 3D video stream and the change of the desired view for a client. Simulation results manifest that our protocol effectively reduces the bandwidth consumption and increases the probability for each client to successfully playback the desired view in a multi-view 3D video.

VII. CoRR

To investigate the case where user subscribes a consecutive sequence of views, we adopt the following setting. User subscribes views according to a Zipf distribution, which means the k th view is subscribed with probability $\frac{c}{(k \bmod m)^s}$ independently to other views. Figure 7 depicts this scenario using $m = 5$ as an example. Following theorem serves as a counterpart of theorem 2 in our main article.

Theorem 3. *In the consecutive view subscription scenario as described above, the ratio $\tilde{\alpha}$ of expected number of views that can be received or synthesized to the number of total subscribed views tends to*

$$p \frac{\sum_{j=1}^m \sum_{x=1}^R \left[\left(\sum_{l=1}^{m-j} \frac{c}{(j+l)^s} + \left(\sum_{t=1}^m \frac{c}{t^s} \right) \frac{x-(m-j)}{m} \right) + \sum_{l=1}^{x-(m-j)} \sum_{x=1}^R \sum_{n=1}^m \left[\left(\sum_{l=1}^{m-j} \frac{c}{(j+l)^s} \right) p \left(\frac{1-p}{(j+l)^s} \right)^{x-1} + \left(\sum_{t=1}^m \frac{c}{t^s} \right) \frac{x-(m-j)}{m} \right] \right]}{\sum_{l=1}^m \frac{c}{l^s}} \quad (9)$$

as $|\mathcal{K}_i| \rightarrow \infty$, where $p = 1 - \prod_{c \in C_i, r \in D_i} \sum_n p_{c,r}^{AP}(n) p_{i,c,r}^n$

Proof: We follow a similar arguments in our main article, which derives the theorem by reward theory. This time, however, we should use a generalized reward process, the Markov reward process. Let T_n denote the index of the n -th successfully received view, and G_n denote the state of the embedded Markov chain, which represents the "position" of the n -th renewal cycle. An example of this definition is represented in figure. 7, in which the states of the first, second and the third cycles are 1, 1, 4 respectively.

The transition probability of G_n is

$$p_{ij} \begin{cases} \frac{p(1-p)^{j-i-1}}{1-(1-p)^m}, & 1 \leq i < j \leq m \\ \frac{p(1-p)^{m-i+j-1}}{1-(1-p)^m}, & 1 \leq j \leq i \leq m \end{cases} \quad (10)$$

since, for example $1 \leq i < j \leq m$, the position change from i to j occurs if and only if there are $j-i$ plus a multiple of m views between the nearest two successfully received views, which means

$$p_{ij} = p(1-p)^{j-i-1} + p(1-p)^{j-i-1+m} + p(1-p)^{j-i-1+2m} + \dots$$

The $\{(G_n, T_n), n = 1, 2, 3, \dots\}$ so defined is then a Markov renewal process.

If we define the reward function of the process as

$$\rho(j, x) = \begin{cases} \sum_{l=1}^x \mathbf{1}(\text{view in the } l \text{ position has been subscribed}), & x \leq m \\ 0, & x \notin \{1, 2, \dots, m\} \end{cases}$$

then

$$Z_\rho = \sum_{n: T_{n+1} < t} \rho(G_n, T_{n+1} - T_n) + \rho(G(t), X(t)) \quad (12)$$

is a Markov reward process, where $X(t)$ is the age process and $G(t)$ be the semi-Markov process associated with our interested Markov renewal process $\{(G_n, T_n), n = 1, 2, 3, \dots\}$. The process so defined as the following desired property: The process just defined has a direct relation to our desired quantity $\tilde{\alpha}$, which is

$$\tilde{\alpha} = \frac{EZ_\rho}{S_t}$$

where S_t is the number of views subscribed by the user. We now intend to apply the theorem 4.1 in [27] to the right hand side of the above equation. In the following, we will use the same notations as in the article just mentioned.

$$\begin{aligned} h(j) &= \sum_{x=1}^{\infty} \rho(j, x) \sum_{j=1,2,\dots} P(G_{n+1} = j, T_{n+1} - T_n = x | G_n = i) \\ &= \sum_{x=1}^{\infty} \rho(j, x) p(1-p)^{x-1} \\ &\quad + \sum_{l=1}^{[x-(m-j)] \bmod m} \left[\left(\sum_{l=1}^{m-j} \frac{c}{(j+l)^s} \right) p \left(\frac{1-p}{(j+l)^s} \right)^{x-1} + \left(\sum_{t=1}^m \frac{c}{t^s} \right) \frac{x-(m-j)}{m} \right] \end{aligned} \quad (13)$$

Observe that the steady state of the chain G_n is uniform distribution, which means

$$\pi_i = \frac{1}{m} \quad (14)$$

Now apply theorem 4.1 in [27], we have

$$\mathbb{E}Z_\rho(t) = pt \sum_{j=1,2,\dots} \pi_j h(j) + o(t)$$

Hence,

$$\frac{\mathbb{E}Z_\rho(t)}{S_t} \rightarrow mp \frac{\sum_{j=1,2,\dots} \pi_j h(j)}{\sum_{l=1}^m \frac{c}{l^s}}$$

$$= p \frac{\sum_{j=1}^m \sum_{x=1}^R \left[\left(\sum_{l=1}^{m-j} \frac{c}{(j+l)^s} + \left(\sum_{t=1}^m \frac{c}{t^s} \right) \frac{x-(m-j)}{m} + \sum_{l=1}^m \frac{c}{l^s} \right) x - \sum_{l=1}^m \frac{c}{l^s} \right]}{\sum_{l=1}^m \frac{c}{l^s}}$$

REFERENCES

- [1] IEEE, "Information Technology–Telecommunications and Information Exchange between Systems Local and Metropolitan Area Networks–Specific Requirements Part 11: Wireless LAN Medium Access Control (MAC) and Physical Layer (PHY) Specifications," *IEEE Standard*, Mar. 2012.
- [2] Y. Mori *et al.*, "View Generation with 3D Warping Using Depth Information for FTV," *Signal Processing: Image Communication*, vol. 24, no. 1-2, pp. 65–72, Jan. 2009.
- [3] B. Oztas *et al.*, "A Rate Adaptation Approach for Streaming Multiview Plus Depth Content," in *IEEE International Conference on Computing, Networking and Communications*, Feb. 2014, pp. 1006–1010.
- [4] M. Nasralla *et al.*, "Bandwidth Scalability and Efficient 2D and 3D Video Transmission over LTE Networks," in *IEEE International Conference on Communications*, Jun. 2013, pp. 617–621.
- [5] B. Feitor *et al.*, "Objective Quality Prediction Model for Lost Frames in 3D Video over TS," in *IEEE International Conference on Communications*, Jun. 2013, pp. 622–625.
- [6] I. Feldmann *et al.*, "HHI Test Material for 3-D Video," *Proc. 84th Meet. ISO/IEC JTC1/SC29/WG11, document M15413*, Apr. 2008.
- [7] Y. Liu *et al.*, "A Novel Rate Control Technique for Multiview Video plus Depth based 3D Video Coding," *IEEE Trans. on Broadcasting*, vol. 57, no. 2, pp. 562–571, 2011.
- [8] F. Shao *et al.*, "Asymmetric Coding of Multi-View Video plus Depth based 3D Video for View Rendering," *IEEE Trans. on Multimedia*, vol. 14, no. 1, pp. 157–167, Feb. 2012.
- [9] N. Chen *et al.*, "Study on Relationship between Network Video Packet Loss and Video Quality," in *4th International Congress on Image and Signal Processing*, Oct. 2011, pp. 282–286.
- [10] A. Hamza and M. Hefeeda, "Energy-Efficient Multicasting of Multiview 3D Videos to Mobile Devices," *ACM Trans. on Multimedia Computing, Communications, and Applications*, vol. 8, no. 3s, pp. 45:1–45:25, Sep. 2012.
- [11] Y. Aksoy *et al.*, "Interactive 2D-3D Image Conversion for Mobile Devices," in *IEEE International Conference on Image Processing*, Sep. 2012, pp. 2729–2732.
- [12] C.-W. Bao and W. Liao, "Performance Analysis of Reliable MAC-layer Multicast for IEEE 802.11 Wireless LANs," in *IEEE International Conference on Communications*, vol. 2, May 2005, pp. 1378–1382.
- [13] A. Sheth *et al.*, "Packet Loss Characterization in WiFi-Based Long Distance Networks," in *IEEE International Conference on Computer Communications*, May 2007, pp. 312–320.
- [14] J. Feng *et al.*, "Wireless Channel Loss Analysis - a Case Study using WiFi-Direct," in *International Wireless Communications and Mobile Computing Conference*, Aug. 2014, pp. 244–249.
- [15] A. Bose and H. F. Chuan, "A Practical Path Loss Model for Indoor WiFi Positioning Enhancement," in *International Conference on Information, Communications and Signal Processing*, Dec. 2007, pp. 1–5.
- [16] S. Keranidis *et al.*, "Contention and Traffic Load-Aware Association in IEEE 802.11 WLANs: Algorithms and Implementation," in *International Symposium on Modeling and Optimization in Mobile, Ad Hoc and Wireless Networks*, May 2011, pp. 334–341.
- [17] "Information Technology–Dynamic Adaptive Streaming over HTTP (DASH)," *ISO/IEC 23009-1*, Dec. 2014.
- [18] IEEE, "Information Technology–Telecommunications and Information Exchange between Systems–Local and Metropolitan Area Networks–Specific Requirements–Part 2: Logical Link Control," *IEEE Standard*, 1998.
- [19] T. Speakman *et al.*, "PGM Reliable Transport Protocol Specification," *IETF RFC 3208*, Dec. 2001.
- [20] H. Schwarz *et al.*, "Overview of the Scalable Video Coding Extension of the H.264/AVC Standard," *IEEE Trans. on Circuits and Systems for Video Technology*, vol. 17, no. 9, pp. 1103–1120, Sep. 2007.
- [21] A. Vetro *et al.*, "Overview of the Stereo and Multiview Video Coding Extensions of the H.264/MPEG-4 AVC Standard," in *Proceedings of the IEEE*, vol. 99, no. 4, Apr. 2011, pp. 626–642.
- [22] G. Cheung *et al.*, "On Dependent Bit Allocation for Multiview Image Coding with Depth-Image-Based Rendering," *IEEE Trans. on Image Processing*, vol. 20, no. 11, pp. 3179–3194, Dec. 2011.
- [23] P. Ndjiki-Nya *et al.*, "Depth Image-Based Rendering with Advanced Texture Synthesis for 3D Video," *IEEE Trans. on Multimedia*, vol. 13, no. 3, pp. 453–465, Jun. 2011.
- [24] C.-H. Lin *et al.*, "Multicast Group Management for Multi-View 3D Videos in Wireless Networks," *CoRR*, vol. abs/1409.8352, 2014.
- [25] S. M. Ross, *Stochastic Processes*, 2nd ed. Wiley, 1983.
- [26] B. Cain *et al.*, "Internet Group Management Protocol, ver. 3," *IETF RFC 3376*, Oct. 2002.
- [27] A. R. Soltani and K. Khorshidian, "Reward processes for semi-markov processes: asymptotic behaviour," *Journal of Applied Probability*, vol. 35, no. 4, pp. 833–842, 12 1998.

